Powder Technology 448 (2024) 120275

Contents lists available at ScienceDirect

Powder Technology

journal homepage: www.journals.elsevier.com/powder-technology

Significant size change during bacterial cellulose capsule drying

Maryam Hosseini, Patrick T. Spicer *

School of Chemical Engineering, University of New South Wales, Sydney, NSW, Australia

HIGHLIGHTS

- Drying of microcapsules with sparse fiber mesh walls is studied.
- Significant shrinkage via capillary stresses collapses the minimal mass capsules.
- The fiber mesh shells can completely recover from huge deformation if rehydrated.

GRAPHICAL ABSTRACT

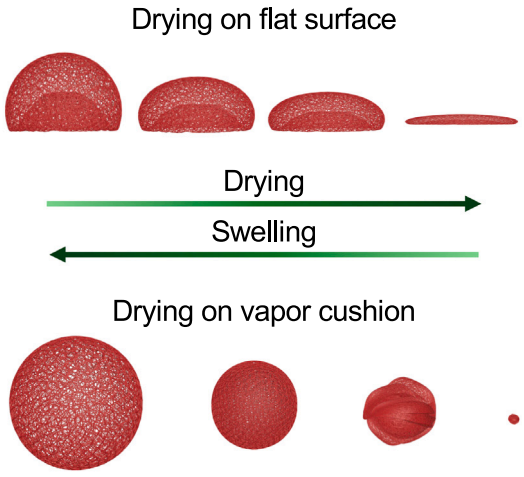

ARTICLE INFO

Keywords:
Fiber
Capsule

ABSTRACT

Use of engineered powders, whether by manufacturers or consumers, often requires rapid hydration but is hindered if hydration rates exceed dispersion rates, leading to "fish eyes". More work is needed to understand how powder could be engineered to actively contribute to its own dispersion while minimizing the use of additional materials and additives. A recently developed bacterial cellulose microcapsule matrix, with good mechanical integrity but minimal mass usage, exhibits remarkable deformability owing to its fibrous shell structure. When dried into powder, the cellulose microcapsules experience significant deformation of their fibrous shells, changing their diameter by orders of magnitude. We demonstrate a capsule shape recovery mechanism by coating the cellulose fibers, which damps fiber interactions. The results demonstrate that drying microfibrous cellulose microcapsules can expand the range of encapsulation modes available and greatly reduce the mass needed to provide efficient powder rehydration.

Introduction

We are pleased to contribute to this Special Issue honoring Dr. Reg Davies, whose broad and enduring impact on particle and powder technology in both industrial and academic settings has been an inspiration to our careers. Of his many areas of expertise, the creation and engineering of powders was of particular concern because of its economic importance to many commercial particulate products. Properties like antimicrobial activity, charge dissipation, and attrition resistance are all important success criteria for engineered powders [1]. We focus here

* Corresponding author.
E-mail address: p.spicer@unsw.edu.au (P.T. Spicer).

https://doi.org/10.1016/j.powtec.2024.120275
Received 1 August 2024; Accepted 10 September 2024
Available online 20 September 2024

on a similarly important aspect of powders: the need to be reconstituted or rehydrated rapidly by various users.

Powders are central to numerous industrial products and processes, and dried particles are commonly engineered to have multiple properties that benefit the most important aspect of their subsequent use by customers: rehydration and reconstitution. Many powders are produced by spray-drying, yielding porous particles that are sometimes post-processed by agglomeration to form granules. Whatever form is used, powders are valuable for their use of minimal materials and rapid rehydration. Limitations in dispersion speed and homogeneity can lead to agglomeration and "fish eye" formation, when powders hydrate faster than they are dispersed [2].

Because of this, rehydration of powders is often the focus of formulation and engineering development efforts. An example is the use of distintegrants, additives used in pharmaceutical powders that aid in hydration and dispersion by swelling coatings, bindings, or added polymer hydrogels [3,4]. There are still opportunities to build on these developments, increase understanding of mechanisms of enhanced hydration, and develop new techniques and additives to provide these benefits.

We show here a way to impart unique swelling capability using stored elasticity in a dried capsule matrix. Instead of synthetic polymers, we use microfibrous cellulose as a matrix that can store elastic energy, expanding by several orders of magnitude in volume upon rehydration, despite using minimal mass and without significant damage. We envision these structures as a way to simultaneously enhance powder formulation and rehydration while avoiding polymers and additives that are facing increased pressures due to sustainability regulations and microplastic bans [5].

Recently, Song et al. [6] developed a soft and flexible microcapsule with an elastic modulus $\sim 100\,\mathrm{Pa}$ that is resistant to fluid shear stresses and large osmotic pressure differences due to its highly porous shell structure. Unlike past capsules made of solid cross-linked or crystalline shells, the microfibrous cellulose capsule shells are made from interwoven fibers, creating a mesh-like shell with an average pore size of $500\,\mathrm{nm}$. The sparse shell structure means even millimeter- or micron-scale capsules can have extremely low solid mass, and possess high water-holding capacity in their core and mesh shell due to cellulose hydroxyl groups [7]. Although such structures are vastly more permeable than typical dense capsule shells, their unusually low density suggests they could significantly alter their shape and permeability during drying and shrinkage, with some similarities to natural pollen grains [8].

The bacterial cellulose microcapsules can undergo extreme deformation during dehydration due to their low-density mesh structure. Capillary pressures squeeze the fibers together tightly enough to seal and deform the capsules [9], while van der Waals interactions between cellulose fibers lead to permanent adhesion and deformation [6,10]. This study explores the implications of these deformation phenomena in cellulose microcapsules being dried by various methods. We examine the drying and reswelling of the microcapsules on different substrates to control capsules' dried shape, size, and porosity, demonstrating orders of magnitude changes in capsule volume by simple drying. A simple surface modification is used to make the drying process reversible, and we study the kinetics of drying and rehydration, as well as the forces involved in shape change during these processes, using imaging measurements. We study these capsules here without significant contents to understand the resilience of the matrix to extreme deformations during drying. It is hoped that these materials could benefit more complex powder particle design, reconstitution, and response.

Methods and materials

Bacterial cellulose microcapsule preparation: Capsules are prepared following the work of Song et al. [6]. First, *Acetobacter xylinum* (Nourishme Organics, Australia) was purified by gradient centrifugation and dispersed in a fermentation culture containing coconut water (Cocobella, Indonesia), 10 wt% of sugar, and 0.5 wt% of Ammonium phosphate (AJAX chemicals, Australia). Then, a gelled oil suspension medium was prepared by mixing $2.5\,\mathrm{g}$ of hydrogenated castor oil (Acme Hardesty) into $100\,\mathrm{mL}$ of canola oil (Coles, Australia) at $90\,^{\circ}\mathrm{C}$ for 10 min. Upon cooling, the organogelator crystallizes and the oil medium develops a yield stress that can suspend water droplets of bacterial culture.

Cellulose microcapsules form as the *Acetobacter xylinum* produce nanocellulose fibers at the liquid–liquid interface of their aqueous emulsion droplets, a bio-interfacial templating process. Within two weeks, the bacteria have formed an entangled mesh cellulose shell with a total thickness of $20-50\,\mu\mathrm{m}$ and pore size of $0.5\,\mu\mathrm{m}$ in each droplet [6]. Growth time can be used to tune the capsule wall fiber density but here we fixed the growth time at two weeks.

Cellulose microcapsules were then separated by heating the gelled oil emulsion to $90\,^{\circ}\mathrm{C}$ for $2\,\mathrm{h}$, then soaking in 2 wt% NaOH (Chem-Supply Pty Ltd, Australia) at room temperature for $24\,\mathrm{h}$ to kill and remove the bacteria. The dead bacteria and other impurities were washed out of the cellulose microcapsules by flushing with Milli-Q water at least three times. If desired, the bacterial cellulose microcapsules were surface treated to enable reversible drying and rehydration by dispersing in different concentrations, 0.25, 0.5, or 1 wt%, of aqueous carboxymethyl cellulose (CMC, MW 250000, Sigma Aldrich, Australia) solution.

Freeze-drying Cellulose microcapsules were immersed in liquid nitrogen then transferred to the freeze drier (Labconco FreeZone, 18 L Freeze Drying System with 18 kg Ice Condenser Capacity). Freeze drying was carried out at $-50\,^{\circ}\mathrm{C}$.

Scanning electron microscopy: Scanning electron microscopy, SEM, was used to study the shape, size, and porosity of cellulose microcapsules after drying. An FEI Nova Nano SEM 450 FE-SEM with an accelerating voltage of $5.0\,\mathrm{kV}$ was used for all SEM imaging. Before SEM imaging, samples were snap-frozen in liquid nitrogen, freeze-dried, and coated with a $30\,\mathrm{nm}$ thick platinum layer using a Leica ACE600 sputter coater.

Optical microscopy: Capsules were stained with Congo Red dye to enable fluorescence imaging and contrast of the fiber structures. Confocal microscopy imaging was carried out on a Zeiss LSM 880 microscope with Airy scan using a 63x oil immersion objective, with numerical aperture NA = 1.4.

Low-magnification optical microscopy images were acquired via stereoscope (WILD M3C, Leica, Germany) with 25x and 40x zoom of a 1X objective to enable individual capsule analysis. Motic Images Plus v2.0 software was used to capture digital images with a $1\,\mathrm{s}$ time interval during drying and swelling. ImageJ software was utilized to measure the microcapsule size with time [11]. All measurements were repeated at least five times. The time-dependent drying and swelling data were fitted to a power-law function using the curve fitting tool in MATLAB [12]. Borosilicate glass capillaries, with dimensions $1\,\mathrm{mm}$ OD and $0.5\,\mathrm{mm}$ ID, were pulled into microcapillary tips with a Micropipette Puller (Model P-97, Sutter Instruments).

Results and discussion

Fig. 1a shows a schematic illustration of the production of bacterial cellulose microcapsules. Bacteria in aqueous emulsion droplets gradually form a shell of entangled cellulose fibers because the droplet interface acts as a template. The resulting capsules have the same dimensions as the starting droplets, allowing customization of the final diameter above a lower limit of about $20\,\mu\mathrm{m}$ [6], that allows for bacterial mobility.

Fig. 1b shows a series of image slices taken via confocal microscopy at $30\,\mu\mathrm{m}$ intervals from the bottom of a bacterial cellulose microcapsule stained with Congo red. The images indicate the random packing of

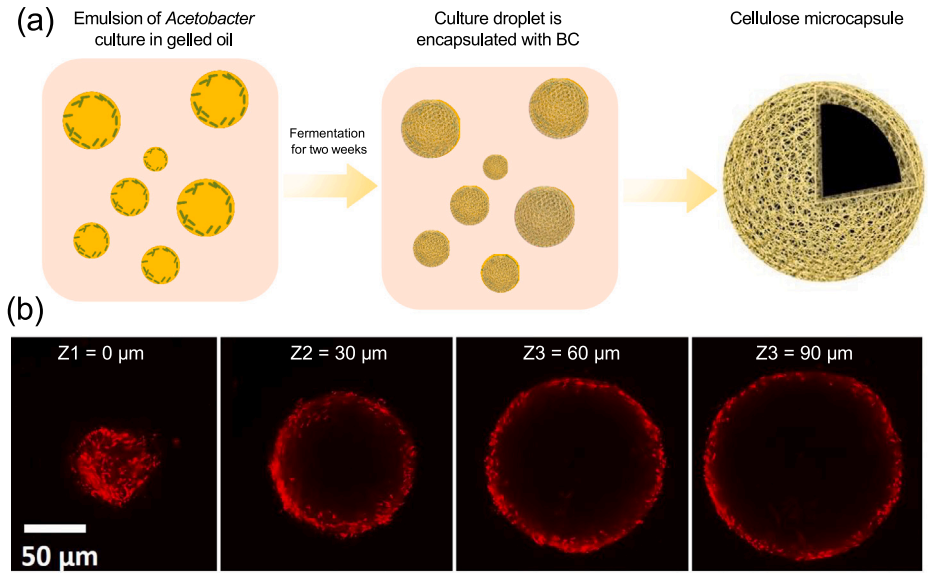

Fig. 1. (a) Schematic illustration of bacterial cellulose microcapsule formation by templating the liquid–liquid interfaces in an emulsion of aqueous bacterial culture droplets dispersed in a gelled oil. (b) Cross-sectional slices taken by confocal microscopy at different z-positions in a cellulose microcapsule with a diameter of 0.15 mm are shown to highlight the fiber density and wall thickness at different z-distances from the capsule surface.

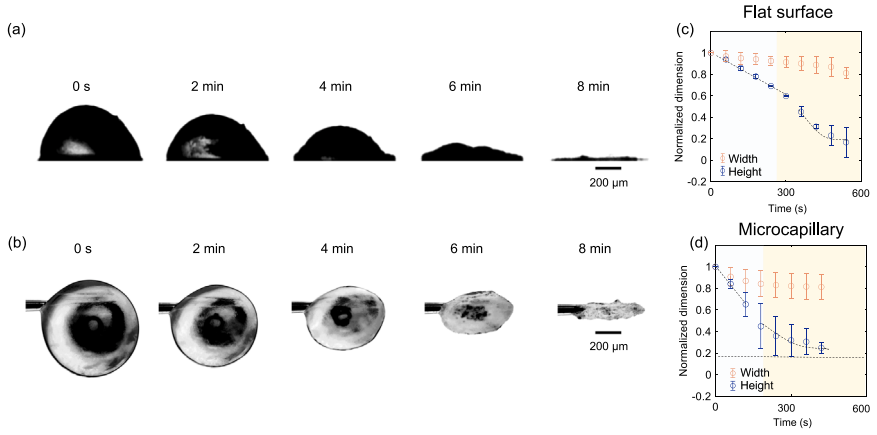

Fig. 2. Time sequence of a cellulose microcapsule viewed from the side as it air dries on (a) a flat glass surface and (b) a cylindrical glass capillary tip. Plots of the change in a drying capsule's width and height over time for ten different capsules on (c) the flat surface and (d) the microcapillary tip, where the dashed line represents the lower limit of shrinkage due to the microcapillary tip dimensions.

the cellulose fibers as well as their sub-micron thickness and lengths on the order of tens of microns. As the slices progress from the bottom the thickness of the wall can be seen to be on the order of 25 µm, with minimal fibers present in the capsule core. These capsules represent a lower bound on the solid mass needed to create a mechanically stable capsule, as the images in Fig. 1b indicate the capsule is almost entirely empty space.

The fibrous mesh structure of the capsule shell has a low solid density, ~ 1%, providing an unusual degree of flexibility and deformability [6,13], but is still strong enough to hold its shape. We are interested to explore drying of these structures to understand how well their sparse fiber mesh shells withstand stresses common to commercial processes and how well they recover. If the low-density framework can be compressed by capillary stresses during drying, it could offer an opportunity to create much smaller particles, with greatly modified porosity, encapsulation, and structure from the starting mesh, since the starting structures have so much room to shrink. In turn, a large change in volume associated with their re-expansion during hydration could provide benefits to difficult powder rehydration and dispersion processes in foods and other formulated products.

Fig. 2 shows a series of time-lapse, side-view images of millimeter-scale cellulose capsules during air drying at room temperature on (a) a flat glass slide and (b) a tapered cylindrical glass microcapillary tip with a maximum diameter of 100 µm. On the flat surface, the initial lightweight capsule is partially flattened into a hemisphere by the surface tension of the water permeating the capsule and wetting the substrate. The capsule hanging on the capillary remains mostly spherical. The right-hand image in each row shows the final size of the cellulose microcapsule after 8 min of air-drying.

The air-drying process leads to a dramatic change in the capsule size, reducing the millimeter-scale capsule to a thickness at least ten times smaller than the initial height, Fig. 2a. The significant deformation results as the capillary forces remove moisture from the core and pores of the capsule. Despite the extreme vertical compression of the capsule by drying, the final width of the dried disk matches the width of the starting hemispherical droplet. The final particle shape is thus determined by the shape of the initial contact line with the substrate. The capsule dried with a smaller contact line on a cylindrical capillary tip wraps around the surface entirely, Fig. 2b, but with a similar level of compression to that on the flat surface. Control of the drying process can thus be achieved by altering the shape of the contact line pinning

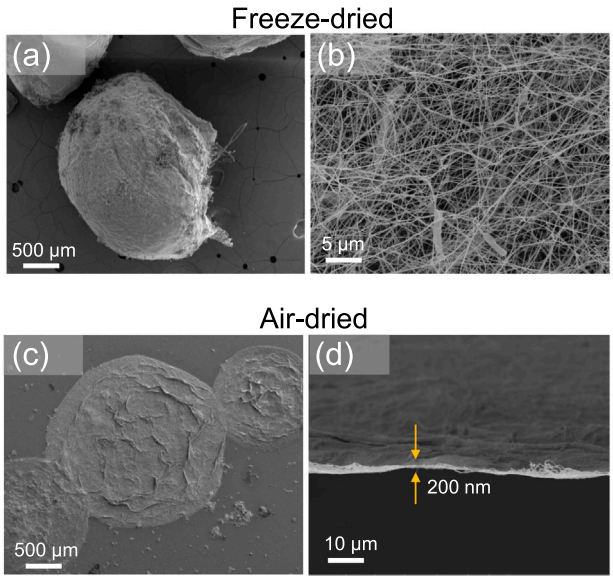

Fig. 3. Scanning electron microscopy (SEM) of cellulose microcapsules after freeze-drying and air-drying. The full capsule is visible in (a) at low magnification and in close-up in (b) for the freeze-dried sample. The air-dried sample is shown from a low-magnification top view in (c) and from an edge view in (d) at higher magnification.

the microcapsule to the substrate, analogous to dried films formed from suspensions [14–16]. The significant compression of the porous capsule is caused by the capillary forces during drying, so we next work to quantify the rates of change to better understand evaporation effects on the fiber shell.

Figs. 2c and d quantify the drying-induced changes in capsule maximum height and width, normalized by their initial value, for the two surfaces used in Figs. 2a and b. A relatively linear decrease in height is observed in the early stages of water evaporation, compressing the capsule to half its initial height in about five minutes, Fig. 2c. The white region of Fig. 2c marks the linear drying region. At longer times, the rate slows and the change in height becomes nonlinear, but the final capsule maximum height is still quite low, varying from 1%–20% of its initial height. Variability mostly results from small wrinkles or bumps in the final disk shape, Fig. 2a. The change in width is much smaller, less than 20%, in agreement with previous research on cellulose fiber drying dynamics [17].

Liquid evaporation occurs in two stages. The evaporation starts with bulk water removal, and the rate depends on the microcapsule size or liquid volume as the capsule is filled with water. The initially linear deformation measured for cellulose microcapsules in Figs. 2c and d is due to bulk water evaporation, reducing the cellulose microcapsule size and porosity due to capillary forces. When the cellulose fibers are close to each other or partially exposed, the second drying stage starts. In the second stage, hydrogen-bonded water evaporation takes place over the cellulose surface. Here the capillary tension reaches its maximum value, and vapor diffusion is the main driving force for continued water evaporation [17]. The second stage of drying is slow as the capillary pressure of the water meniscus is the dominant driving force for microcapsule compressional deformation, pulling cellulose fibers tightly together into a more compact structure. If the fiber surfaces are not in any way hindered from close approach, the structure is compressed by capillary forces until fibers are so close to one other that van der Waals forces can then strongly bind the fibers together [18,19].

It is important to emphasize the extreme adaptation possible for these structures. In Fig. 2a the final height plotted in both cases here is roughly 20% of its initial value, but this represents the resolution limit of the microscope used in the time lapse study. We next turn to SEM imaging to better resolve smaller detail below. Fig. 3 shows images of the entire capsules and their close-up structure for two types of drying process. Fig. 3a shows a capsule that has had its structure preserved by being freeze-dried, a process that uses sublimation of water to dry a sample so that we avoid the capillary pressures that normally compress the capsules during drying. Fig. 3b shows a close-up view of the capsule shell and the mesh of nanoscale thickness fibers making up the shell structure [6]. Although low density, the high connectivity of the mesh provides the mechanical integrity needed to hold a stable shape. However, the high porosity of the mesh structure allows for the significant deformations observed during drying. This combination of properties makes these capsules unique in their response to drying processes.

Fig. 3c shows a top view of a capsule dried normally in air. Comparing with the freeze-dried capsule in Fig. 3a, the width is similar but the capsule has clearly dried into a flat disk as a result of the strong capillary pressures experienced. Fig. 3d is a close-up side view of the flattened capsule, where we can see that the thickness of the dried film is actually much smaller than the original capsule dimensions, on the order of 200 nm, Fig. 3. The capsule shell is about 20 μm thick but we know that the wall is less than 1% solid, with the rest being void space [6]. Here we see compression of the three-dimensional capsule wall from a thickness of 20 μm to 200 nm, a 100× reduction in height, consistent with shrinkage during bulk bacterial cellulose mesh drying [20]. If we assume deformation in the other two dimensions is minimal, the 100× compression is roughly consistent with almost all of the void space being removed from the wall during drying. The large amount of empty space in the capsule center, however, produces a much more dramatic change in volume for the overall capsule, taking a 1 mm tall capsule down to 200 nm, a nearly 5000× reduction in linear dimension and a much larger change in volume.

We are also interested in how these capsules respond to more uniform drying stress, rather than the contact line constrained behavior studied above. This is of interest because the highly anisotropic nature of the high aspect ratio fibers that make up the capsule shell mesh structure may make them respond differently to more complex deformation fields, but also because common drying processes like spray drying occur in spherical droplets without a solid contact line.

Spray-drying is a common method of synthesizing dry particles via rapid drying of droplets [20,21], as droplets are sprayed and exposed to hot air without a contact line biasing the process. Previous work showed that the Leidenfrost phenomenon [22,23] is a viable means of studying the dynamics of single droplet drying [20,24–26], as it dries a droplet floated on a layer of water vapor that forms under the droplet on a high-temperature surface. Here a droplet of aqueous cellulose microcapsule dispersion was placed on a preheated hot plate with a temperature of 180 °C. Images of the process were acquired at a rate of two frames per second to allow tracking of the capsule shrinkage after any excess water in the initial droplet has evaporated.

Fig. 4a shows the shrinkage of a single cellulose capsule during Leidenfrost drying. The initially millimeter-size capsule shrinks in diameter 10×, finishing as a 100 μm diameter particle in the final frame after only 40 s. It is worth noting that the shrinkage is not entirely uniform. Some elongation of the capsule is clear around 20 s in Fig. 4a, perhaps indicating the consolidation of the fibers in the shell has reached a mechanical limit where the structure must buckle. The capsule shrinks until all water evaporates, producing a wrinkled and crumpled particle. Similar dynamics of Leidenfrost drying were recorded for five capsules, the images analyzed for capsule dimensions, and the results plotted in Fig. 4b, normalized by their initial value. The error bars show the variations in capsule size over the different experiments.

Similar to the more constrained drying experiments in Fig. 2 capsule drying on a solid substrate, the Leidenfrost results in Fig. 4b also show initially rapid, linear shrinkage with time as water moves from the capsule core to its surface, followed by a slower nonlinear regime related to migration of the remaining water by diffusion [17,27]. The

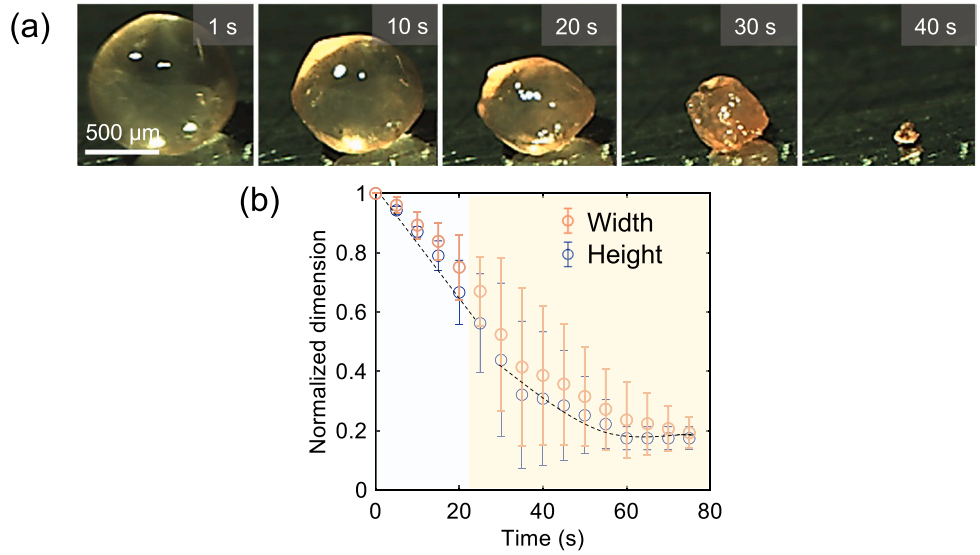

Fig. 4. Compression of cellulose microcapsule without influence of a meniscus or substrate using Leidenfrost phenomena. (a) The microcapsules shrank 1000 times in volume at 180°C. The drying and shrinkage kinetics of five microcapsules are shown in (b), where the capsules shrink in all dimensions until they are ten times smaller their original size.

absence of contact of the droplet with a solid surface means the drying process compresses the capsule more uniformly. Different experimental conditions like temperature, droplet size, and hotplate hydrophobicity can determine the water evaporation rate and final fate of the Leidenfrost drop [22,23], here we only study the final shape as a result of continuous water evaporation to distinguish from pinned drying conditions.

In addition to the shrinkage observed in Fig. 4, we find evidence that the fiber mesh structure consolidates distinctly during Leidenfrost drying versus capsules dried on a surface. Two different behaviors are seen: continuous shrinkage to a smaller capsule [20,24–26] and shrinkage followed by overpressure/explosion. Overpressure behavior has been seen before for droplets dried with a solute present and are distinguished by the production of an audible cracking sound during the explosion [22–24]. If the capsule is able to build sufficient pressure to explode, it must mean that the formerly porous fiber mesh has consolidated and sealed itself strongly during drying. We examine the structures of two capsules dried via Leidenfrost drying more closely using SEM imaging below.

Fig. 5 shows SEM images of cellulose microcapsules after dehydration using the Leidenfrost effect. The capsule in Fig. 5a was able to release the internal pressure faster than it could build during compression, possibly due to a small hole in its wall prior to drying. As a result, the capsule collapsed and experienced buckling and bending [17,27,28]. Fig. 5c shows a close-up view of the wall of the capsule in Fig. 5a and the significant wrinkling that occurred during drying. Buckled structures are also produced by spray drying processes of slurries or solutions when droplets are converted into particles or capsules [24,25].

If pressure cannot be relieved via leakage, the capsule will overpressurize and explode to relieve the pressure, as occurred for the capsule in Fig. 5b. For water at 180 °C the steam pressure is 0.8 MPa, much larger than the cellulose microcapsule modulus. The close-up view of the exploded capsule wall in Fig. 5d is significantly different from the one in Fig. 5c. Here the fibers appear to be tightly consolidated and the fracture surface has ruptured the shell so that jagged points are visible. We speculate that the more uniform shrinkage that occurs during Leidenfrost drying brings more fibers together along their edges, creating much more contact area and strength in the compact. If so, it is not surprising that pressure inside the capsule can build and reach levels high enough to eventually rupture the structure.

In all the above instances, capsule drying is an irreversible process because of strong fiber–fiber interactions at small distances. As a result,

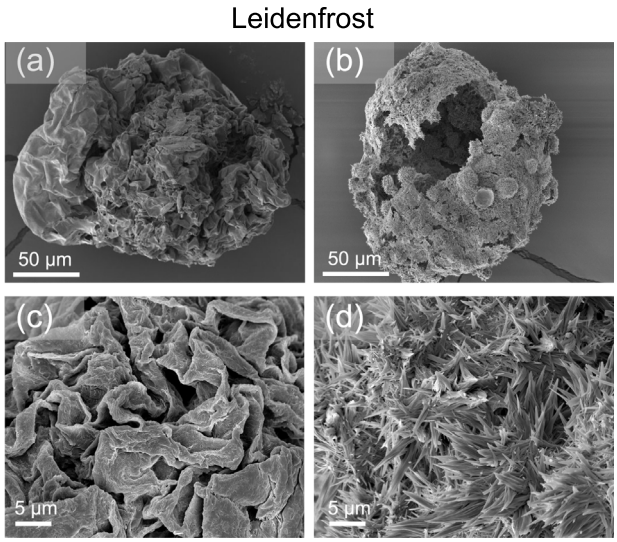

Fig. 5. Scanning electron microscopy of cellulose microcapsules after Leidenfrost drying. Two types of dried structures form, (a) shrunken and (b) wrinkled shells. Close-ups of the structures formed under these conditions show the (c) buckling that occurs to accommodate the shrinkage of the shell in (a) and (d) the fractured areas that form where the fibers have sealed the droplet and overpressurized in the capsule in (b).

rehydration to recover the original much larger shape is impossible. We can, however, also dry these capsules in a way that allows them to rehydrate and regain their initial form by modifying the cellulose surface with adsorbed polymer to mitigate the strong fiber interactions. A number of different materials can be used, simply by mixing the cellulose capsules with a solution of the surface modifier. A commonly used example is the anionic polymer carboxymethyl cellulose, CMC, that has a strong affinity for cellulose surfaces [29,30]. Three concentrations of CMC are used, 0.25%, 0.5%, and 1% w/w. Fig. 6a shows a time sequence of a cellulose microcapsule, previously equilibrated in 1 wt% aqueous CMC solution, drying in air. As in Fig. 2, the spherical capsule is compressed into a hemispherical shape that gradually flattens as the water evaporates. In this case, the water leaves behind the cellulose capsule made of fibers that are now coated with CMC that prevents the fibers from irreversibly binding. Despite the additional component

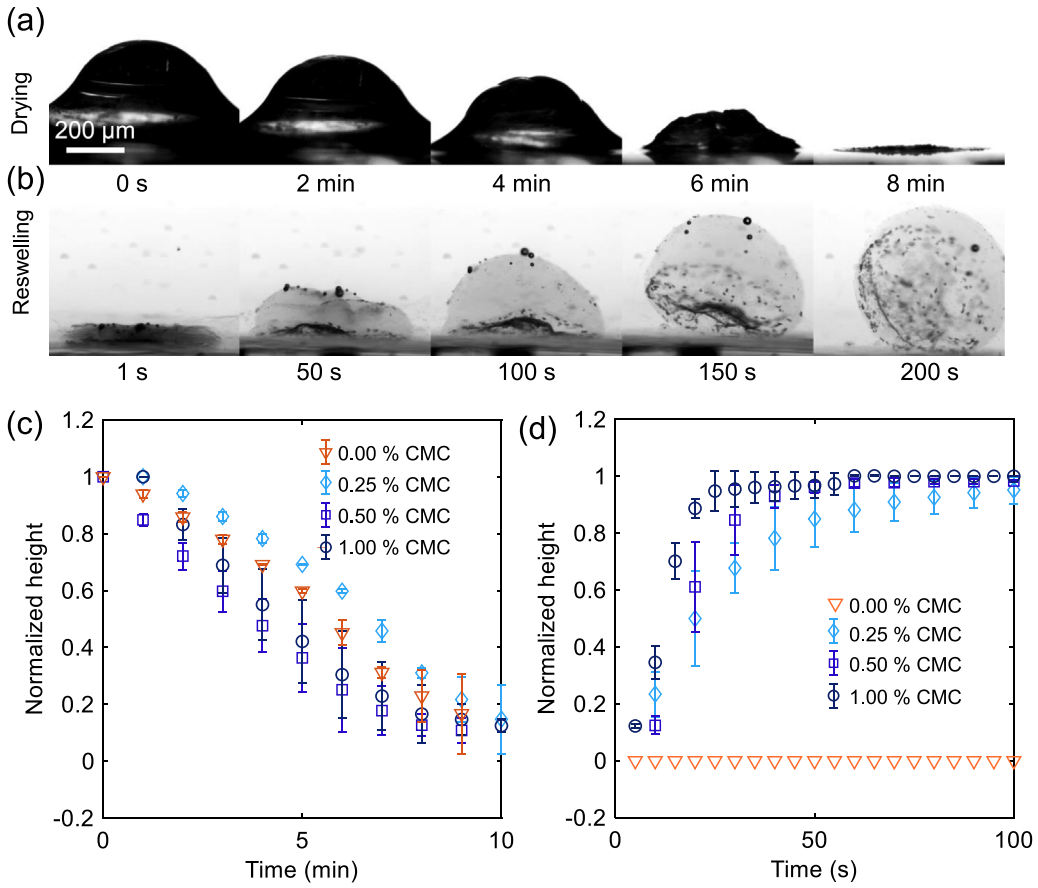

Fig. 6. (a) Cellulose microcapsule-CMC drying in air on a glass slide. (b) Swelling on the dried cellulose microcapsule-CMC in water. (c) Kinetics of cellulose microcapsule-CMC air dehydration at room temperature, and (d) Swelling kinetics of dried cellulose microcapsule-CMC in water at room temperature. Here the microcapsule height is normalized by the initial microcapsule height.

present, the flattened disk formed by drying is still a tiny fraction of the capsule's original height.

When placed in water, however, the cellulose-CMC capsule rehydrates rapidly, as shown in Fig. 6b. The capsule goes from a thin disk only microns high to a spherical capsule roughly 0.5 mm tall. The sparse nature of the capsule shell is visible here, with the back wall of the capsule partially seen through the front surface. These capsules appear to have a nice balance of strength and flexibility, making them an interesting matrix to consider for encapsulation or simply reinforcement of powder particles. The fiber structures can withstand amazing levels of compression but still regain their original shapes as long as they do not strongly adhere when dried.

The dynamics of the cellulose-CMC capsule drying, Fig. 6c, exhibit similar behavior to those dried without CMC present, Fig. 2 and Fig. 4. The capsule shrinkage rate decreased with increasing CMC concentration, probably as a result of increased fluid viscosity at higher CMC concentrations. The dynamic recovery of the capsule shape during rehydration also follows a cycle of initially rapid change and then slower relaxation, though the initial time scale is on the order of seconds rather than minutes. Increasing CMC concentration increases the recovery speed but does not impact the degree to which the capsule ultimately recovers. No recovery is observed for the capsules that had no CMC treatment, as the fibers are permanently bound together during drying. The simple addition of a polymer surface modifier enables control of the drying and redispersion process for these sparse fiber capsule structures, allowing a wide range of functional responses to be designed.

Conclusions

In this study, we have quantified the drying-induced shrinkage of capsules made of bacterial cellulose microfiber mesh. Drying significantly deforms the cellulose microcapsule as a result of its minimal mass content, converting an initially millimeter-scale capsule into flattened structures with thicknesses that can get down to the sub-micron scale. The capsules' relatively low elastic modulus and mesh structure enables large changes in volume during air-drying and the drying process is strongly affected by the contact line forces on a given surface. The Leidenfrost method of drying particles is used to shrink the millimeter-scale capsules without a substrate effect by drying the capsule on a vapor layer. Doing so creates truly shrunken capsules, rather than flattened shapes. The drying process is found to be reversible if the cellulose fiber surfaces are first treated with polymer additives that prevent fibers from contacting closely and irreversibly bonding. The sparse cellulose mesh can thus act as a powder scaffold that adds structure and preserves form with minimal mass usage. If drying is reversible by rehydration, the powder gains an important additional function: shape-memory and local stress response. The significant volume change upon rehydration enables the creation of powders that expand sufficiently to potentially contribute to their dispersion and the prevention of "fish eye" formation.

CRediT authorship contribution statement

Maryam Hosseini: Investigation, Methodology, Writing – original draft, Writing – review & editing. **Patrick T. Spicer:** Conceptualization, Funding acquisition, Investigation, Methodology, Supervision, Writing – original draft, Writing – review & editing.

Declaration of competing interest

The authors declare that they have no known competing financial interests or personal relationships that could have appeared to influence the work reported in this paper.

Data availability

Data will be made available on request.

Acknowledgments

Confocal microscopy and scanning electron microscopy were performed using instruments in the Katharina Gaus Light Microscopy Facility (KGLMF) and Electron Microscope Unit (EMU) at the Mark Wainwright Analytical Centre (MWAC), UNSW Sydney. MH acknowledges support from a UNSW Scientia PhD fellowship. PS acknowledges partial support from the Australian Government through the Australian Research Council's Discovery Projects funding scheme, Project DP190102614, the Linkage Projects funding scheme, Project LP200201026, and the Linkage Infrastructure, Equipment and Facilities (LIEF) funding scheme, Project LE200100221.

References

[1] R. Davies, G.A. Schurr, P. Meenan, R.D. Nelson, H.E. Bergna, C.A. Brevett, R.H. Goldbaum, Engineered particle surfaces, Adv. Mater. 10 (15) (1998) 1264–1270.
[2] P. Methacanon, C. Gamonpilas, A. Kongjaroen, C. Buathongjan, Food polysaccharides and roles of rheology and tribology in rational design of thickened liquids for oropharyngeal dysphagia: A review, Compr. Rev. Food Sci. Food Saf. 20 (4) (2021) 4101–4119.
[3] P. Gould, S. Tan, The effect of recompression on the swelling kinetics of wet massed tablets, containing 'super' disintegrants, Drug Dev. Ind. Pharmacy 11 (9–10) (1985) 1819–1836.
[4] G. Bolhuis, K. Zuurman, G. Te Wierik, Improvement of dissolution of poorly soluble drugs by solid deposition on a super disintegrant. II. The choice of super disintegrants and effect of granulation, Eur. J. Pharmaceut. Sci. 5 (2) (1997) 63–69.
[5] E. Kentin, H. Kaarto, An EU ban on microplastics in cosmetic products and the right to regulate, Rev. Eur., Compar. Int. Environ. Law 27 (3) (2018) 254–266.
[6] J. Song, F. Babayekhorasani, P.T. Spicer, Soft bacterial cellulose microcapsules with adaptable shapes, Biomacromolecules 20 (12) (2019) 4437–4446.
[7] D.E. Ciolacu, Structure-property relationships in cellulose-based hydrogels, J.: Polym. Polym. Compos.: Ref. Ser. Cellul.-Based Superabsorbent Hydrogels (2018) 1–32.
[8] E. Katifori, S. Alben, E. Cerda, D.R. Nelson, J. Dumais, Foldable structures and the natural design of pollen grains, Proc. Natl. Acad. Sci. 107 (17) (2010) 7635–7639.
[9] L.D. Landau, E.M. Lifšic, E.M. Lifshitz, A.M. Kosevich, L.P. Pitaevskii, Theory of Elasticity: Volume 7, vol. 7, Elsevier, 1986.
[10] L. Salmén, J.S. Stevanic, Effect of drying conditions on cellulose microfibril aggregation and "hornification", Cellulose 25 (11) (2018) 6333–6344.
[11] C.A. Schneider, W.S. Rasband, K.W. Eliceiri, NIH Image to ImageJ: 25 years of image analysis, Nat. Methods 9 (7) (2012) 671–675.
[12] The MathWorks, Inc., Curve Fitting Toolbox, Natick, Massachusetts, United State, 2020, URL https://www.mathworks.com/products/curvefitting.html.
[13] M. Hosseini, F. Babayekhorasani, Z. Guo, K. Liang, V. Chen, P.T. Spicer, Propulsion, deformation, and confinement response of hollow nanocellulose millimotors, J. Colloid Interface Sci. 628 (2022) 435–445.
[14] K.N. Al-Milaji, H. Zhao, New perspective of mitigating the coffee-ring effect: Interfacial assembly, J. Phys. Chem. C 123 (19) (2019) 12029–12041.
[15] Y. Li, Q. Yang, M. Li, Y. Song, Rate-dependent interface capture beyond the coffee-ring effect, Sci. Rep. 6 (1) (2016) 1–8.
[16] M. Talantikite, N. Leray, S. Durand, C. Moreau, B. Cathala, Influence of arabinoxylan on the drying of cellulose nanocrystals suspension: From coffee ring to maltese cross pattern and application to enzymatic detection, J. Colloid Interface Sci. 587 (2021) 727–735.
[17] Y. Peng, D.J. Gardner, Y. Han, Drying cellulose nanofibrils: in search of a suitable method, Cellulose 19 (1) (2012) 91–102.
[18] C.C.N. Martins, M.C. Dias, M.C. Mendonça, A.F.S. Durães, L.E. Silva, J.R. Félix, R.A.P. Damásio, G.H.D. Tonoli, Optimizing cellulose microfibrillation with NaOH pretreatments for unbleached Eucalyptus pulp, Cellulose 28 (18) (2021) 11519–11531.
[19] S. Sinquefield, P.N. Ciesielski, K. Li, D.J. Gardner, S. Ozcan, Nanocellulose dewatering and drying: current state and future perspectives, ACS Sustain. Chem. Eng. 8 (26) (2020) 9601–9615.
[20] R. de Souza Lima, M.-I. Ré, P. Arlabosse, Drying droplet as a template for solid formation: A review, Powder Technol. 359 (2020) 161–171.
[21] A.B.D. Nandiyanto, K. Okuyama, Progress in developing spray-drying methods for the production of controlled morphology particles: From the nanometer to submicrometer size ranges, Adv. Powder Technol. 22 (1) (2011) 1–19.
[22] D. Quéré, Leidenfrost dynamics, Annu. Rev. Fluid Mech. 45 (2013) 197–215.
[23] S. Lyu, V. Mathai, Y. Wang, B. Sobac, P. Colinet, D. Lohse, C. Sun, Final fate of a leidenfrost droplet: Explosion or takeoff, Sci. Adv. 5 (5) (2019) eaav8081.
[24] Y. Sugiyama, R.J. Larsen, J.-W. Kim, D.A. Weitz, Buckling and crumpling of drying droplets of colloid- polymer suspensions, Langmuir 22 (14) (2006) 6024–6030.
[25] N. Tsapis, E.R. Dufresne, S.S. Sinha, C.S. Riera, J.W. Hutchinson, L. Mahadevan, D.A. Weitz, Onset of buckling in drying droplets of colloidal suspensions, Phys. Rev. Lett. 94 (1) (2005) 018302.
[26] A. Yarin, G. Brenn, O. Kastner, C. Tropea, Drying of acoustically levitated droplets of liquid–solid suspensions: Evaporation and crust formation, Phys. Fluids 14 (7) (2002) 2289–2298.
[27] N. Alhajj, N.J. O'Reilly, H. Cathcart, Designing enhanced spray dried particles for inhalation: A review of the impact of excipients and processing parameters on particle properties, Powder Technol. 384 (2021) 313–331.
[28] E. Lintingre, F. Lequeux, L. Talini, N. Tsapis, Control of particle morphology in the spray drying of colloidal suspensions, Soft Matter 12 (36) (2016) 7435–7444.
[29] S.J. Veen, A. Kuijk, P. Versluis, H. Husken, K.P. Velikov, Phase transitions in cellulose microfibril dispersions by high-energy mechanical deagglomeration, Langmuir 30 (44) (2014) 13362–13368.
[30] S.J. Veen, P. Versluis, A. Kuijk, K.P. Velikov, Microstructure and rheology of microfibril–polymer networks, Soft Matter 11 (46) (2015) 8907–8912.